High-Frequency Open Boundary Condition of Transient Seepage Equation

S. Prempramote[1,*]

[1] *Department of Civil Engineering, Faculty of Engineering, Kasetsart University, Bangkok, Thailand*

Abstract

A high-frequency open boundary condition has been developed for transient seepage analyses of an isotropically saturated soil layer with a constant depth. The boundary condition of the open boundary is derived in the frequency domain by adopting the continued fraction technique. The coefficients of the continued fraction solution are determined recursively at the high-frequency limit. By introducing auxiliary variables and the high-frequency continued fraction solution to the prescribed seepage flow of water-pore water pressure relationship in the frequency domain, the open boundary condition is eventually in terms of a system of fractional differential equations after transformed to the time domain. No convolution integral is required. The accuracy of the analysis results increases with the increasing order of the continued fraction.

Keywords: seepage, pore water pressure, open boundary condition, continued fraction, dynamic stiffness

1. Introduction

In numerical modeling of unbounded domains, the domains are usually truncated somewhere to specify their far field boundaries with fixed or free boundary conditions due to their very large areas. Such boundary conditions imposed in the modeling often lead to spurious reflections at the truncated boundaries when transient analyses of the domains are carried out. As a result, the solutions obtained from the analyses are numerically polluted. Several approaches were hence proposed and have been continuously developed to cope with such a problem, such as the boundary element method (BEM) [1-3], the infinite elements [4-6], the scaled boundary finite element method (SBFEM) [7-8], absorbing boundary conditions (ABCs) implemented in the finite element method (FEM) [9-12], and the perfectly matched layer (PML) that is able to attenuate propagating waves [13-14], etc. These approaches are able to satisfy the boundary condition at infinity, in other words, the radiation condition.

Apart from such approaches, there is another interesting one, the high-order transmitting boundary, which is based on use of the continued fraction technique [15]. The transmitting boundary was introduced to study the displacement responses of semi-half spaces under dynamic loads at high frequencies. Its boundary condition is expressed as a system of first-order differential equations in the time domain. The distinct advantage of the boundary is that it can be implemented with FEM. Therefore time-step schemes are applicable to the time-domain analysis, and the convolution integral, which is a computationally expensive task, is no longer required. Soon after, the doubly asymptotic open boundaries were developed from such a transmitting boundary using the same continued fraction technique, but extending to the low-frequency expansion [16-17]. The boundaries are specifically applicable to full-planes with a circular cavity and semi-infinite layers with a constant depth [18].

One of the important problems in the modeling of unbounded domains is seepage flow of groundwater since the pore water pressure generated in soil mass may significantly affect existing structures such as tunnels, dams, etc. Some of the mentioned approaches were also developed for transient seepage analyses in infinite media, for example, the finite element method with cloning cell technique [19], the infinite element using the hydraulic head distribution function [20], and the infinite element using the analytical solution of a one-dimensional axially symmetric configuration [21].

The objective of the paper is thus aimed at developing a high-order open boundary condition used for transient seepage analyses of a semi-infinite layer with a constant depth under short-time and long-time seepage

* Corresponding author

E-mail address: fengsype@ku.ac.th

flow of water to study the responses of pore water pressure. The unbounded domain used in the analyses is herein assumed to be an isotropically saturated soil with a constant depth.

2. Dynamic Stiffness of Unbounded Domain

For an isotropically saturated soil, the governing equation of two-dimensional transient seepage is expressed as a second-order differential equation,

$$\nabla^2 u = \frac{1}{c}\dot{u} \tag{1}$$

where the pore water pressure $u = u(x,z,t)$, the Laplace operator $\nabla^2 = \partial^2/\partial x^2 + \partial^2/\partial z^2$ and c denotes the coefficient of consolidation. The arguments of functions are omitted herein for simplicity in the nomenclature. The initial condition of the unbounded domain initially at rest is given as

$$u = \gamma_w z \qquad (0 \le z \le d,\ t = 0) \tag{2}$$

where γ_w is the unit weight of water and d is the depth of the soil layer. The geometry and boundary conditions of the soil layer are given in subsection 2.1. By employing the method of separation of variables, Eq.(1) can be transformed to a series of one-dimensional transient seepage equations. From a two-dimensional transient seepage equation and the definition of a dynamic stiffness coefficient, an equation of the dynamic stiffness coefficient can be derived.

2.1 Saturated soil layer with constant depth

An isotropically saturated soil layer with a constant depth d as shown in Fig. 1 represents an unbounded domain of which the right-hand boundary extends to infinity. For convenience, the x-axis of the coordinate system is chosen at the upper boundary Γ_U of the layer. The formulation of the proposed open boundary condition is based on the dynamic stiffness representing the property of the soil layer. It is dependent of the coordinate system. The boundary conditions of the soil layer are as follows: at the upper boundary Γ_U ($z = 0$), $u = 0$ for $0 < t < \infty$, while at the lower boundary Γ_L ($z = d$), $u = u_0$ for $t = 0$, and the vertical boundary Γ_V ($0 \le z \le d$), $\dot{u} = 0$ for $t = 0$.

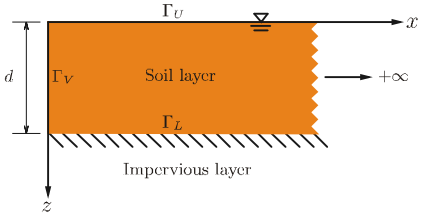

Fig. 1. Saturated soil layer with constant depth

Equation(1) is also expressed in the frequency domain as

$$U_{,xx} + U_{,zz} - \frac{1}{c}(\mathrm{i}\omega)U = 0 \tag{3}$$

where the amplitude of pore water pressure $U = U(x,z,\omega)$, the unit imaginary number $i = \sqrt{-1}$, and ω denotes the excitation frequency. The solutions of Eq.(3) can be determined using the method of separation of variables as expressed in the following equation:

$$U = XZ \tag{4}$$

where $X = X(x,\omega)$ and $Z = Z(z)$. Substituting Eq.(4) into Eq.(3) and multiplying the equation by d^2 yield

$$d^2 \frac{X_{,xx}}{X} - (\mathrm{i}a_0) = -d^2 \frac{Z_{,zz}}{Z} \tag{5}$$

where the dimensionless frequency is defined as

$$a_0 = \frac{\omega d^2}{c} \tag{6}$$

It is necessary that both sides of Eq.(5) must be equal to the same constant, which is denoted as λ^2. Hence, Eq.(5) can be separated into the following two equations:

$$Z_{,zz} + \left(\frac{\lambda}{d}\right)^2 Z = 0 \tag{7}$$

$$X_{,xx} - \frac{1}{d^2}((\mathrm{i}a_0) + \lambda^2)X = 0 \tag{8}$$

The solutions of Eq.(7) are in the form of

$$Z = C_1 \cos\left(\frac{\lambda}{d}z\right) + C_2 \sin\left(\frac{\lambda}{d}z\right) \tag{9}$$

where C_1 and C_2 are constants. At $z = 0$, the boundary condition is $u = 0$. This implies that Z in Eq.(4) must be equal to zero. As a result, C_1 in Eq.(9) is zero while C_2 is arbitrary. C_2, however, never be calculated and is negligible. Therefore, Eq.(9) can be reduced to the eigenfunction,

$$Z_j = \sin\left(\frac{\lambda_j}{d}z\right) \qquad (j = 0,\ 1,\ 2,\ \ldots) \tag{10}$$

which are the nontrivial solutions of Eq.(7), where

$$\lambda_j = \frac{(2j+1)\pi}{2} \tag{11}$$

The index j denotes a mode number. This implies that λ in Eq.(8) varies with each mode. For the one-dimensional seepage equation (Eq.(8)), its solution that satisfies the boundary condition at infinity is given in the form of modal pore water pressure amplitude,

$$X_j = C_j e^{-\sqrt{(\mathrm{i}a_0)+\lambda_j^2}\,x/d} \tag{12}$$

where C_j is a constant. The prescribed seepage flow amplitude of each mode $Q_j = Q_j(x,\omega)$ on the vertical boundary at arbitrary x is expressed as

$$Q_j = -dX_{j,x} \tag{13}$$

Substituting Eq.(12) into Eq.(13) in turn yields

$$C_j = \left(\sqrt{(\mathrm{i}a_0)+\lambda_j^2}\, e^{-\sqrt{(\mathrm{i}a_0)+\lambda_j^2}\,x/d} \right)^{-1} Q_j \tag{14}$$

By substituting Eqs.(10) and (12) back into Eq.(4), and using Eqs.(11) and (14), the solution of each mode is expressed as

$$U_j = \left(\sqrt{(\mathrm{i}a_0)+\lambda_j^2} \right)^{-1} Q_j \sin\left(\frac{\lambda_j}{d} z \right) \tag{15}$$

An alternative way to determine X_j can be done by introducing the dynamic stiffness coefficient $S^{\infty}_j = S^{\infty}_j(a_0)$ to the prescribed seepage flow of water-pore water pressure relationship,

$$X_j = \left(S_j^{\infty} \right)^{-1} Q_j \tag{16}$$

, which is equivalent to the force-displacement relationship as derived in [16]. Substituting Eq.(13) into Eq.(16) yield

$$X_{j,x} = -\frac{1}{d} S_j^{\infty} X_j \tag{17}$$

Differentiating Eq.(17) with respect to x and substituting Eq.(17) to the differentiated equation lead to

$$X_{j,xx} = \frac{1}{d^2} \left(S_j^{\infty} \right)^2 X_j \tag{18}$$

Substituting Eq.(18) into Eq.(8) and eliminating X_j in the equation the dynamic stiffness equation of each mode j yield

$$\left(S_j^{\infty} \right)^2 - (\mathrm{i}a_0) - \lambda_j^2 = 0 \tag{19}$$

The solution of Eq. (19) can be determined as

$$S_j^{\infty} = \sqrt{(\mathrm{i}a_0)+\lambda_j^2} \tag{20}$$

Only the positive root is chosen to satisfy the boundary condition at infinity. By substituting Eqs.(10) and (16) back into Eq.(4), and using Eq.(20), the solution of each mode is expressed as similar as Eq.(15),

$$U_j = \left(\sqrt{(\mathrm{i}a_0)+\lambda_j^2} \right)^{-1} Q_j \sin\left(\frac{\lambda_j}{d} z \right) \tag{21}$$

The solution in the time domain of either Eq.(15) or Eq.(21) after expressed in the frequency domain can be determined using the convolution integral,

$$u_j = \int_0^t s_j^{-1} q_j \, d\tau \tag{22}$$

where the pore water pressure $u_j = u_j(t)$, the flexibility coefficient $s_j^{-1} = (s_j(t-\tau))^{-1}$ and the prescribed seepage flow of water $q_j = q_j(\tau)$.

2.2 High-frequency continued fraction solution

This section describes the solution of the dynamic stiffness equation for modal dynamic stiffness coefficient (Eq.(20)). The solution is sought as a high-frequency continued fraction solution. Only one step is involved in the solution procedure i.e. a continued fraction solution is determined at the high-frequency limit recursively. In each recursion, the coefficients of one term of the continued fractions is obtained, and an equation is established for the residual. For simplicity in the derivation, the modal index subscript j is omitted in this section. The continued fraction solution at the high-frequency limit is written as

$$S^{\infty} = K_{\infty} - (\mathrm{i}a_0)(Y^{(1)})^{-1} \tag{23a}$$

$$Y^{(i)} = Y_0^{(i)} - (\mathrm{i}a_0)(Y^{(i+1)})^{-1} \qquad (i = 1,\ 2,\ 3,\ \ldots,\ M_H) \tag{23b}$$

where K_{∞} and $Y_0^{(i)}$ are coefficients to be determined recursively in the solution procedure. $(\mathrm{i}a_0)(Y^{(1)})^{-1}$ and $(\mathrm{i}a_0)(Y^{(i+1)})^{-1}$ are the residual terms where $Y^{(i)} = Y^{(i)}(a_0)$ and $Y^{(i+1)} = Y^{(i+1)}(a_0)$. M_H is the order of the continued fraction solution at a high frequency. The coefficient K_{∞} is determined by substituting Eq.(23a) into Eq.(20). This leads to an equation of a power series of $(\mathrm{i}a_0)$, including the following two terms:

$$(K_{\infty}^2 - \lambda^2) - (\mathrm{i}a_0)(1 + 2K_{\infty}(Y^{(1)})^{-1} - (\mathrm{i}a_0)(Y^{(1)})^{-2}) = 0 \tag{24}$$

This equation is satisfied by setting all the terms equal to zero. Thus the solution for K_{∞} that satisfies the boundary condition at infinity is obtained from the first term (constant term) by selecting the positive root. Thus,

$$K_{\infty} = \lambda \tag{25}$$

The last term of Eq.(24) is an equation of $Y^{(1)}$. After being multiplied by $(Y^{(1)})^2$ and substituted with Eq.(25), the last term becomes

$$(Y^{(i)})^2 + b_0^{(i)} Y^{(\mathrm{i})} - (\mathrm{i}a_0)c^{(i)} = 0 \tag{26}$$

with the introduced constants

$$b_0^{(1)} = 2\lambda \tag{27}$$

$$c^{(1)} = 1 \tag{28}$$

for the case of $i = 1$. To begin the recursive procedure, Eq.(23b) with $i = 1$ must be substituted into Eq.(26). This also results in an equation of a power series of $(\mathrm{i}a_0)$ grouped into the following two terms:

$$((Y_0^{(i)})^2 + b_0^{(i)} Y_0^{(i)}) - (\mathrm{i}a_0)(c^{(i)} + b_0^{(i)}(Y^{(i+1)})^{-1} + 2Y_0^{(i)}(Y^{(i+1)})^{-1} - (\mathrm{i}a_0)(Y^{(i+1)})^{-2}) = 0 \tag{29}$$

Equation(29) is also satisfied by setting all the two terms equal to zero. The non-zero solution of the first term (constant term) is

$$Y_0^{(i)} = -b_0^{(i)} \tag{30}$$

The last term of Eq.(29) is an equation of $Y^{(i+1)}$. After being multiplied by $(Y^{(i+1)})^2$ and substituted with Eq.(30), the last term becomes the recursive equation used in the high-frequency limit,

$$(Y^{(i+1)})^2 + b_0^{(i+1)} Y^{(i+1)} - (\mathrm{i}a_0)c^{(i+1)} = 0 \tag{31}$$

with the introduced constants

$$b_0^{(i+1)} = -\frac{b_0^{(i)}}{c^{(i)}} \tag{32}$$

$$c^{(i+1)} = \frac{1}{c^{(i)}} \tag{33}$$

The high-frequency continued fraction solution in Eq.(23a) is constructed from the solutions of the constants K_∞ in Eq.(25) and $Y_0^{(i)}$ in Eq.(30). For example, the high-frequency continued fraction solution with the order $M_H = 3$ can be written as

$$S^\infty = K_\infty - \cfrac{(\mathrm{i}a_0)}{Y_0^{(1)} - \cfrac{(\mathrm{i}a_0)}{Y_0^{(2)} - \cfrac{(\mathrm{i}a_0)}{Y_0^{(3)}}}} \tag{34}$$

2.3 High-frequency open boundary condition

The high-frequency open boundary condition in the frequency domain is constructed using the relationship between the prescribed seepage flow amplitude Q and modal pore water pressure amplitude X as expressed below

$$Q = S^\infty X \tag{35}$$

where S^∞ denotes a continued fraction solution using Eqs.(23a) and (23b) in the previous subsection. Afterwards, substituting Eq.(23a) into Eq.(35) leads to

$$Q = K_\infty X - (\mathrm{i}a_0)^{1/2} X^{(1)} \tag{36}$$

where the introduced auxiliary variable $X^{(1)}$ is defined as

$$X^{(1)} = (\mathrm{i}a_0)^{1/2} (Y^{(1)})^{-1} X \tag{37}$$

Rearrange Eq. (37) as

$$(\mathrm{i}a_0)^{1/2} X = Y^{(1)} X^{(1)} \tag{38}$$

which is as similar as the form in Eq.(35). Similarly, an auxiliary variable is introduced for each term of the continued fraction in Eq.(23b). This results in

$$(\mathrm{i}a_0)^{1/2} X^{(i)} = Y^{(i+1)} X^{(i+1)} \qquad (i = 0,\ 1,\ 2,\ \ldots,\ M_H) \tag{39}$$

where Eq.(38) is included as the case of $i = 0$ with $X^{(0)} = X$. Multiplying Eq.(23b) by $X^{(i)}$ and using the definition of auxiliary variables in Eq.(39) formulated with i and $i - 1$ result in

$$(\mathrm{i}a_0)^{1/2} X^{(i-1)} = Y_0^{(i)} X^{(i)} - (\mathrm{i}a_0)^{1/2} X^{(i+1)} \qquad (i = 1,\ 2,\ 3,\ \ldots,\ M_H) \tag{40}$$

The residual $X^{(M_H+1)}$ of an order M_H high-frequency continued fraction solution is approximated as zero. Equations(36) and (40) are all combined to form a matrix equation,

$$([K_h] + (\mathrm{i}\omega)^{1/2}[C_h])\{\tilde{X}\} = \{\tilde{Q}\} \tag{41}$$

where $\{\tilde{X}\} = [X,\ X^{(1)},\ \ldots,\ X^{(M_H)}]^T$ and $\{\tilde{Q}\} = [Q,\ 0,\ \ldots,\ 0]^T$ while the time-independent matrices

$$[K_h] = \begin{bmatrix} K_\infty & & & & \\ & Y_0^{(1)} & & & \\ & & Y_0^{(2)} & & \\ & & & \ddots & \\ & & & & Y_0^{(M_H)} \end{bmatrix} \tag{42}$$

$$[C_h] = \frac{d}{\sqrt{c}} \begin{bmatrix} & -1 & & & \\ -1 & & -1 & & \\ & -1 & & \ddots & \\ & & \ddots & & -1 \\ & & & -1 & \end{bmatrix} \tag{43}$$

The function $\{\tilde{X}\}$ includes the modal pore water pressure amplitude X on Γ_V and all the auxiliary variables $(X^{(1)},\ \ldots, X^{(M_H+1)})$ and the only non-zero entry at the right-hand side $\{\tilde{Q}\}$ includes the prescribed seepage flow amplitude of water Q. Note that Eq.(6) is substituted into the equation to replace $(\mathrm{i}a_0)$ with $(\mathrm{i}\omega)$. The matrix $[K_h]$ is diagonal while the matrix $[C_h]$ is banded and symmetric. Equation(41) can be transformed into the open boundary condition in the time domain as the following equation:

$$[K_h]\{\tilde{x}\} + [C_h]D^p\{\tilde{x}\} = \{\tilde{q}\} \tag{44}$$

where $\{\tilde{x}\} = [x,\ x^{(1)},\ \ldots,\ x^{(M_H)}]^T$, $\{\tilde{q}\} = [q,\ 0,\ \ldots,\ 0]^T$ and $D^p = d^p/dt^p$ is the fractional derivative operator of order p which is equal to 1/2. The vector $\{\tilde{x}\}$ can be solved by employing the improved numerical method of Riemann-Liouville fractional derivative [22] in association with

the Newmark's method using the average acceleration scheme as expressed in the following steps:

step 1: solve for $\{\tilde{x}\}_{n+1}$ in the following equation:

$$\{\tilde{x}\}_{n+1} = \left([K_h] + \frac{\gamma \Delta t^{-p}}{\beta(1-p)(2-p)\Gamma(1-p)} [C_h] \right)^{-1} \times \left(\{\tilde{q}\}_{n+1} - \frac{\Delta t}{\Gamma(1-p)} [C_h] (\frac{1}{2} t_n^{-p} \{\tilde{x}\}_0 + \frac{1}{2} \Delta t^{-1/2} \{\dot{\tilde{x}}\}_n + \sum_{k=1}^{n-2} (t_{n+1} - k\Delta t)^{-1/2} \{\dot{\tilde{x}}\}_{k\Delta t}) + \frac{\Delta t^{1-p}}{(1-p)(2-p)\Gamma(1-p)} [C_h] \times (\frac{\gamma}{\beta \Delta t} \{\tilde{x}\}_n + (p - 2 + \frac{\gamma}{\beta}) \{\dot{\tilde{x}}\}_n + (\frac{\gamma}{2\beta} - 1) \Delta t \{\ddot{\tilde{x}}\}_n) \right) \quad (45)$$

step 2: solve for $\{\ddot{\tilde{x}}\}_{n+1}$ in the following equation:

$$\{\ddot{\tilde{x}}\}_{n+1} = \frac{1}{\beta(\Delta t)^2} (\{\tilde{x}\}_{n+1} - \{\tilde{x}\}_n - \Delta t \{\dot{\tilde{x}}\}_n) - (\frac{1}{2\beta} - 1) \{\ddot{\tilde{x}}\}_n \quad (46)$$

using $\{\tilde{x}\}_{n+1}$ from Eq.(45);

step 3: solve for $\{\dot{\tilde{x}}\}_{n+1}$ in the following equation:

$$\{\dot{\tilde{x}}\}_{n+1} = \{\dot{\tilde{x}}\}_n + (1-\gamma)\Delta t \{\ddot{\tilde{x}}\}_n + \gamma \Delta t \{\ddot{\tilde{x}}\}_{n+1} \quad (47)$$

using $\{\ddot{\tilde{x}}\}_{n+1}$ from Eq. (46). Note: n is the time station and the gamma function $\Gamma(1-p) = \sqrt{\pi}$, and the constants γ and β are 0.5 and 0.25, respectively.

3. Numerical Examples

For simplicity in the analyses, the ratios of d^2/c is assumed to be equal to 1 through all the examples.

3.1 Example 1

In the first example, the testing of the open boundary condition at a high-frequency mode is carried out. The mode $j = 1000$ with $\lambda = 2001(\pi/2)$ is selected as such a high-frequency mode. The prescribed seepage flow of water is chosen as an impulse function as shown in Fig. 2(a) of which the Fourier transform is displayed in Fig. 2(b). The highest dimensionless frequency of interest is observed as 150.

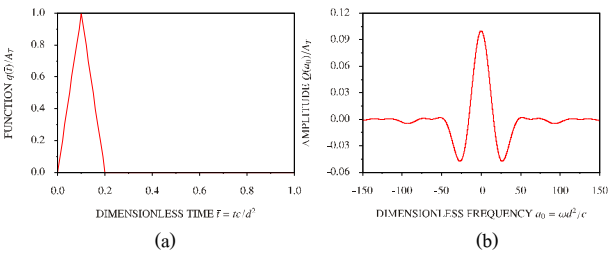

(a) (b)

Fig. 2. Prescribed seepage flow of water as impulse function: (a) time history and (b) Fourier transform

In the frequency-domain analysis, the analysis result obtained from the continued fraction solution of dynamic stiffness (Eq.(23a)) using $M_H = 1$ is plotted as real and imaginary parts with respect to the dimensionless frequency a_0 as shown in Figs. 3(a) and 3(b), respectively. For the real part, the obtained result becomes a straight line, intersecting the y-axis at 1, whereas that of the imaginary part is an inclined line with a very low gradient, intersecting the origin. In comparison with the exact solution of dynamic stiffness (Eq.(20)), the continued fraction solution performs well since the curves of the real and imaginary parts of the solution fit those of the exact solution.

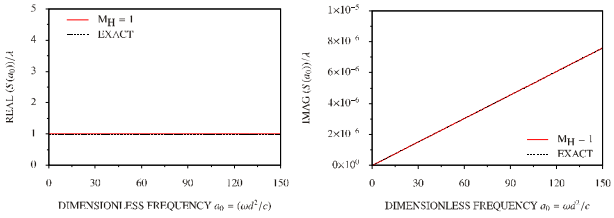

(a) (b)

Fig. 3. High-frequency continued fraction solution with $M_H = 1$ for modal dynamic stiffness ($\lambda = 2001(\pi/2)$) : (a) real part and (b) imaginary part

In the time-domain analysis, the time step Δt used for the convolution integral (Eq.(22)) and the open boundary condition (Eq.(44)) with $M_H = 1$ is selected as 0.02 to gain the accurate responses of pore water pressure. The responses obtained from the convolution integral and the open boundary condition are plotted in Fig. 4. The responses are normalized by the seepage flow amplitude A_T with respect to the dimensionless time $\bar{t}$, which is equal to tc/d^2. It can be seen that the response curve obtained from the open boundary condition with merely $M_H = 1$ fits the response curve obtained from the convolution integral throughout the entire range.

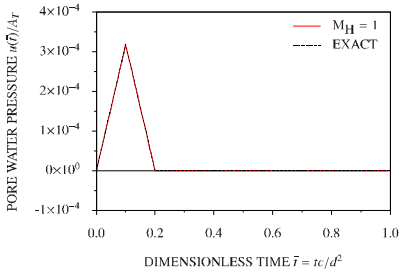

Fig. 4. Modal response of pore water pressure ($\lambda = 2001(\pi/2)$) by high-frequency open boundary condition with $M_H = 1$

3.2 Example 2

The mode $j = 1000$ of the first example is still tested in the second example, but the prescribed seepage flow function is changed to be a

harmonic function, $q(\bar{t}) = A_T \sin(2\pi f \bar{t})$, where the amplitude $A_T =$ 1 and the frequency $f = 2.5$ as shown in Fig. 5(a) for the time history and Fig. 5(b) for its Fourier transform. The time step Δt used for the convolution integral and the open boundary condition is reduced to be 0.01 so as to gain the accuracy of the results.

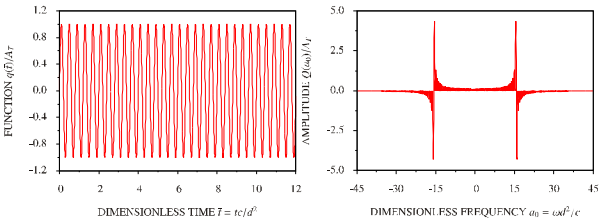

(a) (b)

Fig. 5. Prescribed seepage flow of water as harmonic function: (a) time history and (b) Fourier transform

The response curve of pore water pressure obtained from the open boundary condition with $M_H = 1$ corresponds to that of the exact responses as plotted in Fig. 6(a). When the curve obtained from the open boundary condition is considered closely as zoomed in Fig. 6(b) to 6(d) for three ranges, the curve fits that of the exact response throughout the entire range. Being similar to the first example, the open boundary condition with merely $M_H = 1$ still performs well at the high-frequency mode for the case of harmonic seepage flow of water.

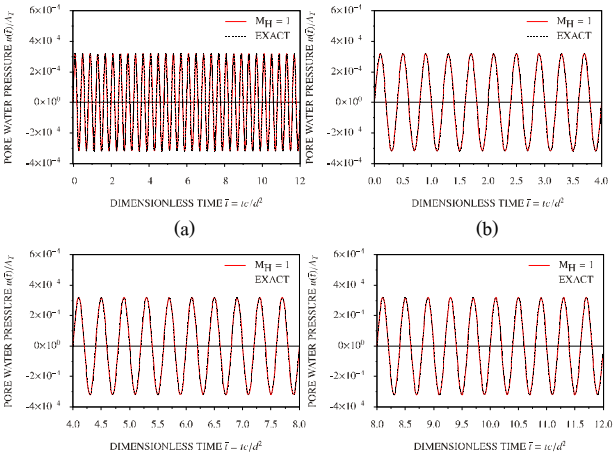

(a) (b) (c) (d)

Fig. 6. Modal response of pore water pressure ($\lambda = 2001(\pi/2)$) by high-frequency open boundary condition with $M_H = 1$: (a) for $0 \le \bar{t} \le 12$, (b) for $0 \le \bar{t} \le 4$, (c) for $4 \le \bar{t} \le 8$, and (d) for $8 \le \bar{t} \le 12$

3.3 Example 3

In the third example, the mode $j = 0$ with $\lambda = \pi/2$, which is a low-frequency mode, is selected for the test. The prescribed seepage flow of water represented by the impulse function used in the first example (see Fig. 2(a)) is re-applied in this example.

In the frequency-domain analysis, the analysis results of the continued fraction solution of dynamic stiffness using $M_H = 1$, 4 and 8 are plotted in Figs. 7(a) and 7(b) for the real and imaginary parts, respectively. For the real part, the result obtained from $M_H = 1$ becomes a straight line, intersecting the y-axis at 1, whereas that of the imaginary part is an inclined line, intersecting the origin. It is perceived that the curve of the continued fraction solution is obviously different from that of the exact solution. However, when the order of continued fraction M_H increases to 4, the accuracy of the continued fraction solution increases as well. Until the order M_H increases up to 8, the continued fraction solution approaches the exact one. In other words, the accuracy of the continued fraction solution increases with the increasing order. Compared to the first two examples at the high-frequency mode, in this example at the low-frequency one, the order of continued fraction used is higher in order to gain more the accurate result.

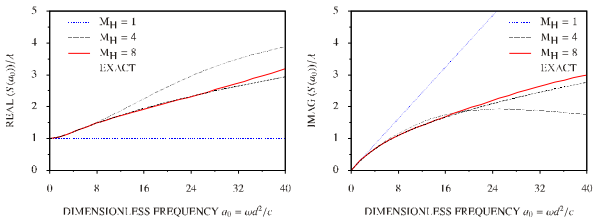

(a) (b)

Fig. 7. High-frequency continued fraction solution with $M_H = 1$, 4 and 8 for modal dynamic stiffness ($\lambda = \pi/2$): (a) real part and (b) imaginary part

In the time-domain analysis, the time step Δt used for the convolution integral and the open boundary condition with $M_H = 1$ is selected as 0.005 to gain the accurate responses of pore water pressure. The analysis results are plotted in Fig. 8. From the obtained results, it is noticed that as the order of continued fraction increases from 1 to 4, the accuracy of the responses also increases. As soon as the order increases up to 8, the response curve almost fits that of the exact response under the impulse seepage flow of water. This shows that a higher order is required for an accurate result in the time-domain analysis at a low-frequency mode.

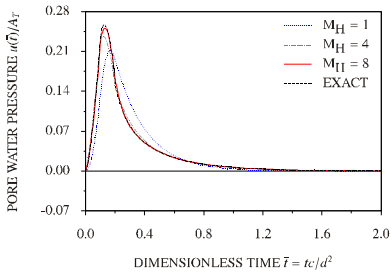

Fig. 8. Modal response of pore water pressure ($\lambda = \pi/2$) by

high-frequency open boundary condition with $M_H = 1$, 4 and 8

3.4 Example 4

In the last example, the low-frequency mode $\lambda = 1$ is selected for the test. The prescribed seepage flow of water under an earthquake (long-time seepage flow) as assumed in Fig. 9(a) with its Fourier transform in Fig. 9(b) is used in this analysis.

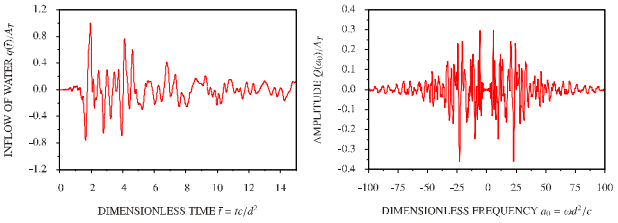

(a) (b)

Fig. 9. Prescribed seepage flow of water under earthquake excitation: (a) time history and (b) Fourier transform

In the frequency-domain analysis, the analysis results obtained from the continued fraction solution of dynamic stiffness using $M_H = 1$, 5 and 10 are plotted in Figs. 10(a) and 10(b) for the real and imaginary parts, respectively. Being similar to the third example, the continued fraction solution approaches the exact one with the increasing order. As the order increases up to 10, the curves of the real and imaginary parts of the continued fraction solution nearly fits those of the exact one.

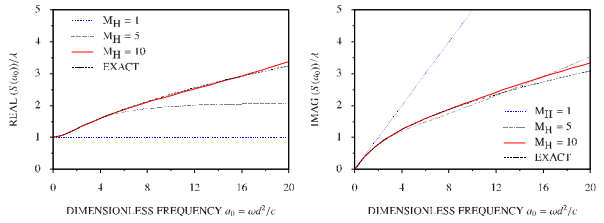

(a) (b)

Fig. 10. High-frequency continued fraction solution with $M_H = 1$, 5 and 10 for modal dynamic stiffness ($\lambda = 1$): (a) real part and (b) imaginary part

In the time-domain analysis, the time step Δt of 0.005 is also used for both the convolution integral and the open boundary condition to gain the accurate responses of pore water pressure. Similarly, the accuracy of the open boundary condition increases with the increasing order of continued fraction as plotted in Fig. 11. It is noted that when the order of continued fraction increases to 5, the response curve is almost the same as that of the convolution integral, except at the turning points (where the slopes are equal to zero); for example as zoomed in Fig. 11(b) for the range of $0 \le \bar{t} \le 5$. However, to obtain the more accurate results for the entire range at the turning points, the order of continued fraction has to increase up to 10 as zoomed in Figs. 11(c) to 11(d). This reveals that the open boundary condition also performs well under earthquake excitation even at a low-frequency mode with use of a higher order.

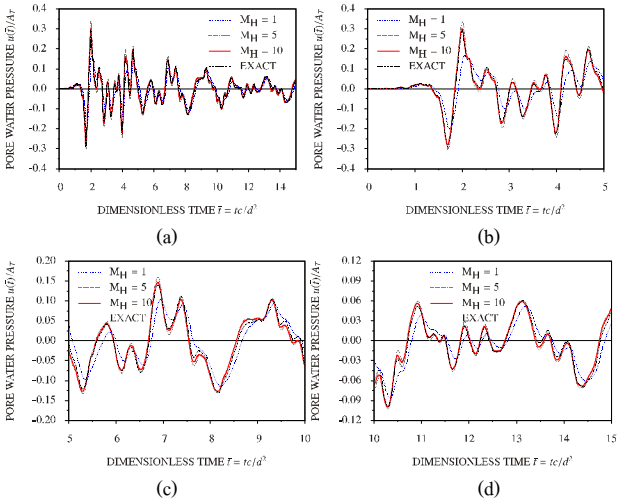

(a) (b)

(c) (d)

Fig. 11. Modal response of pore water pressure ($\lambda = 1$) by high-frequency open boundary condition with $M_H = 1$, 5 and 10: (a) for $0 \le \bar{t} \le 15$, (b) for $0 \le \bar{t} \le 5$, (c) for $5 \le \bar{t} \le 10$, and (d) for $10 \le \bar{t} \le 15$

4. Conclusion

The high-order high-frequency open boundary condition introduced herein is specifically applicable to modal transient seepage equations of isotropically saturated soil layers with a constant depth. The open boundary condition is expressed as a system of fractional differential equations in the time domain.

The two time-independent coefficient matrices, the static stiffness and damping matrices, are diagonal and symmetrically banded, respectively. Therefore, well-established time-stepping schemes in structural dynamics are directly applicable, and convolution integral is no longer required.

As demonstrated in the numerical examples using the impulse, harmonic seepage flow of water and also the seepage flow of water under earthquake excitation, the accuracy of the analysis results in both frequency and time domains increases with the increasing order of continued fraction. The open boundary condition performs well at the high-frequency modes with a low order of continued fraction. Only at the low-frequency modes, a higher order of continued fraction is required to gain an accurate result.

References

[1] P.K. Banerjee and R. Butterfield, "Boundary Element Method in Geomechanics", *Finite Element in Geomechanics*. John Wiley & Sons, New York, pp. 529-570, 1977.

[2] C.A. Brebbia and J. Dominguez. “Boundary element methods for potential problems”. *Applied Mathematical Modelling*, 1, pp. 372-378, 1977.

[3] J. Dominguez. “Stress Analysis around Anchor Plates: a Boundary Element Method Application.” Ph.D. thesis, Universidad de Sevilla, 1977.

[4] P. Bettess and O.C. Zienkiewicz. “Diffraction and refraction of surface waves using finite and infinite elements”. *International Journal for Numerical Methods in Engineering*, 11(8), pp. 1271-1290, 1977.

[5] D.S. Burnett and R.L. Holford. “Prolate and oblate spheroidal acoustic infinite elements”. *Computer Methods in Applied Mechanics and Engineering*, 158(1), pp. 117-141, 1998.

[6] R.J. Astley. “Infinite elements for wave problems: a review of current formulations and an assessment of accuracy”. *International Journal for Numerical Methods in Engineering*, 49(7), pp. 951-976, 2000.

[7] C. Song and J.P. Wolf. “The scaled boundary finite-element method – alias consistent infinitesimal finite-element cell method – for elastodynamics”. *Computer Methods in Applied Mechanics and Engineering*, 147(3-4), pp. 329-355, 1997.

[8] J.P. Wolf and C. Song. “The scaled boundary finite-element method – a primer: derivations”. *Computers & Structures*, 78(1-3), pp. 191-210, 2000.

[9] B. Engquist and A. Majda. “Absorbing boundary conditions for the numerical simulation of waves”. *Mathematics of Computation*, 31(139), pp. 629-651, 1977.

[10] A. Bayliss and E. Turkel. “Radiation boundary conditions for wave-like equations”. *Communications on Pure and Applied Mathematics*, 33(6), pp. 707-725, 1980.

[11] T. Hagstrom, A. Mar-Or and D. Givoli. “High-order local absorbing conditions for the wave equation: extensions and improvements”. *Journal of Computational Physics*, 227(6), pp. 3322-3357, 2008.

[12] E. Bécache, D. Givoli and T. Hagstrom. “High-order absorbing boundary conditions for anisotropic and convective wave equations”. *Journal of Computational Physics*, 229(4), pp. 1099-1129, 2010.

[13] W.C. Chew and O.H. Liu. “Perfectly matched layers for elastodynamics: a new absorbing boundary condition”. *Journal of Computational Acoustics*, 4(4), pp. 341-359, 1996.

[14] F. Collino and C. Tsogka. “Application of the perfectly matched absorbing layer model to the linear elastodynamic problem in anisotropic heterogeneous media”. *Geophysics*, 66(1), pp. 294-307, 2001.

[15] M.H. Bazyar and C. Song. “A continued-fraction-based high-order transmitting boundary for wave propagation in unbounded domains of arbitrary geometry”. “*International Journal for Numerical Methods in Engineering*, 74(2), pp. 209-237, 2008.

[16] S. Prempramote, C. Song, F. Tin-Loi and G. Lin. “High-order doubly asymptotic open boundaries for scalar wave equation”. *International Journal for Numerical Methods in Engineering*, 79(3), pp. 340-374, 2009.

[17] S. Prempramote and C. Song, “A High-Order Doubly Asymptotic Open Boundary Condition for Scalar Waves in a Waveguide”, *2nd International Conference on Computational Methods in Structural Dynamics and Earthquake Engineering (COMPDYN 2009)*, Island of Rhodes, Greece, 2009.

[18] S. Prempramote. “Development of High-Order Doubly Asymptotic Open boundaries for Wave Propagation in Unbounded Domains by Extending the Scaled Boundary Finite Element Method.” Ph.D. thesis, Civil and Environmental Engineering, The University of New South Wales, Sydney, Australia, 2011.

[19] N. Khalili, W. Wang and S. Valliappan, “A finite element cloning method for ground water flow problems in infinite media”, *3rd Asian-Pacific Conference on Computational Mechanics*, Seoul, Korea, 1996, 3, pp. 1849-1857.

[20] C. Zhao and S. Valliappan. “Transient infinite elements for seepage problems in infinite media”. *International Journal for Numerical and Analytical Methods in Geomechanics*, 17(5), pp. 323-341, 1993.

[21] N. Khalili, S. Valliappan and M. Yazdchi. “An axi-symmetric infinite element for transient radial flow problems”. *International Journal for Numerical and Analytical Methods in Geomechanics*, 23(8), pp. 801-813, 1999.

[22] W. Zhang and N. Shimizu, “The improved numerical method of Riemann-Liouville fractional derivative for FE formulation”, *Computational Mechanics WCCM VI in conjunction with APCOM’04*, Beijing, China, 2004.